High-Throughput Zika Viral Titer Assay for Rapid Screening of Antiviral Drugs

Emily M. Lee,[1,2,] Steven A. Titus,[2,*] Miao Xu,[2] Hengli Tang,[1] and Wei Zheng[2]*

[1]*Department of Biological Science, Florida State University, Tallahassee, Florida.*
[2]*National Center for Advancing Translational Sciences, National Institutes of Health, Bethesda, Maryland.*
**These authors contributed equally to this work.*

ABSTRACT

Zika virus has recently emerged as a worldwide pathogen and public health burden due to its rapid spread and identification as a causative agent for multiple neurological defects, including congenital microcephaly. While there has been a flurry of recent research to address this emerging pathogen, there are currently no approved drug treatments for ZIKV infection. The gold standard for testing antiviral activity is to quantify infectious virion production. However, current infectious viral production assays, such as the plaque-forming or focus-forming unit assay, are tedious and labor intensive with a low-screening throughput. To facilitate drug development, we developed a Zika viral titration assay using an automated imaging system and an image analysis algorithm for viral colony quantification. This assay retained the principle of the classical virus titer assay, while improving workflow and offering higher screening throughput. In addition, this assay can be broadly adapted to quantification of other viruses.

Keywords: Zika virus, viral titer assay, compound screening, antiviral, high throughput, focus-forming unit

INTRODUCTION

Zika virus (ZIKV) is a mosquito-borne and sexually transmitted flavivirus with reported vector-borne transmission in ~84 countries, subnational areas, or territories worldwide.[1] The recent re-emergence of ZIKV and its link to neurological disorders, including congenital microcephaly and Guillain–Barré syndrome, have precipitated the need for prompt drug and vaccine development.[2–6] The current gold-standard assay for testing antiviral effects of candidate therapeutics is the quantification of post-treatment infectious virion production, which has the benefit of identifying antiviral compounds with activity at any or multiple stage(s) of the viral life cycle. The gold-standard assay measures plaque-forming or focus-forming units. Because the focus-forming assay (FFA) relies on the direct detection of intracellular viral proteins, this variation has both improved sensitivity and decreased incubation time compared with the classical plaque assay. In addition, noncytotoxic viruses that cannot form plaques may still be quantified in the FFA, provided there is a suitable antibody for immunostaining against the viral antigen.[7] However, these traditional titer assays are typically not suitable for high-throughput drug screening because they are labor intensive, time consuming, and prone to user bias during manual counting. To address these shortcomings, we have developed a semiautomated, high-throughput FFA using an automated imaging workflow. This new system greatly increases the assay throughput and improves reproducibility due to reduction in user subjectivity by employing automation, and can also be broadly adapted to other viruses for titer quantification.

MATERIALS AND METHODS

Materials

Electronic multichannel pipettes and ClipTips™ (E1-ClipTip 12-channel 0.5–12.5 μL, 2–125 μL, 30–850 μL) were purchased from Thermo Fisher Scientific (Waltham, MA). The multichannel (8-channel) Costar® vacuum aspirator was purchased from Millipore-Sigma (Burlington, MA). The glioblastoma SNB-19 cell line was obtained from the U.S. National Cancer Institute 60 human tumor cell line (NCI60). The monkey kidney Vero cell line and *Aedes albopictus* C6/36 cell line were purchased from the American Tissue Culture Collection (ATCC, Manassas, VA). D1-4G2-4-15 hybridoma cells for production of the 4G2 antiflavivirus envelope antibody were also purchased from ATCC. Goat antimouse immunoglobulin G (IgG) horse radish peroxidase (HRP) was purchased from Abcam (Cambridge, United Kingdom). Diaminobenzidine (DAB)-substrate staining kit was purchased from Vector Labs (Burlingame, CA).

Cell Culture

The glioblastoma SNB-19 cell line was maintained at 37°C in 5% CO_2 in RPMI-1640 medium, 1×penicillin–streptomycin-amphotericin B (PSA), and 10% fetal bovine serum (FBS)

   DOI: 10.1089/adt.2018.881

(Thermo Fisher Scientific). The monkey kidney Vero cell line was maintained at 37°C in 5% CO_2 in Dulbecco's modified Eagle's medium (DMEM), 1X penicillin-streptomycin, and 10% FBS. The *Aedes albopictus* C6/36 cell line was maintained at 28°C in 5% CO_2 in Eagle's minimal essential medium (EMEM) (ATCC), penicillin-streptomycin, and 10% FBS.

ZIKV Culture

Zika virus stocks were generated in *Aedes albopictus* clone C6/36 cells from PRVABC59-ZIKV strain stocks (ATCC). To amplify viral stocks, a T-75 flask of C6/36 cells (90%–95% confluency) was inoculated with 1×10^6 Zika virions in low volume (3 mL) for 1 h, with rocking to disperse media every 15 min. After 1 h, 17 mL of media was added, and C6/36 cells were maintained at 28°C in 5% CO_2 for 7 days. At day 7 postviral inoculation, supernatants were harvested, filtered, and stored at −80°C, fresh media added to the day 7 ZIKV-infected C6/36 culture, and supernatant harvested again 24 h later (day 8) postviral inoculation. ZIKV titer was determined by focus-forming unit assay. For SNB-19 cell infections, cells were seeded onto 96-well plates 1 day before viral infection. SNB-19 cells were incubated with compounds for 1 h before addition of high-titer C6/36-derived ZIKV at multiplicity of infection (MOI) = 0.5–1. Compounds were not removed from cells. SNB-19 cell supernatants were then harvested at 24 h postinfection from the 96-well plates, and either frozen at −80°C or used immediately for focus-forming unit assay. Importantly, each experiment included a dimethylsulfoxide titration for normalization to account for any batch-to-batch variation in viral titer.

Compound Dilutions and Viral Inoculation

SNB-19 cells were seeded overnight into 96-well plates to achieve 20,000–30,000 cells the next day. In 96-well compound dilution plates, 300 μL of 1X complete DMEM (DMEM, 10% FBS, 1% PSA, 1% NEAA to row A and 200 μL of 1X complete DMEM) to rows B–H using the ClipTip 30–850 μL multichannel electronic pipet. Individual compounds in a volume of 0.9 μL at 10 mM concentration were added to each well in row A, for a total of 12 compounds per 96-well plate, using the ClipTip 0.5–12.5 μL multichannel electronic pipet. Each well in row A was mixed three times at 100 μL/well using the ClipTip 2–125 μL multichannel electronic pipet. Then, 100 μL was removed from row A, and added to row B and mixed. This process was repeated for each dilution across rows C through G to achieve a 7-fold dilution range of 30–0.03 μM (30, 10, 3, 1, 0.3, 0.1, and 0.03 μM). Row H was the no compound control. Day-old media from SNB-19 cells were removed by aspiration, and 100 μL of each drug dilution was added to the previously seeded SNB-19 cells. After a 1 h incubation at 37°C and 5% CO_2, high-titer Zika virus (<1 μL of strain PRVABC59) was added to cells at MOI = 0.5–1, and incubated for 24 h.

ZIKV Titer Assay

A step-by-step method for the ZIKV titer assay is detailed in Table 1 and illustrated in *Figure 1*. In brief, vero cells were seeded overnight into 96-well plates to achieve a confluent monolayer the next day. Infected SNB-19 supernatant from each drug titration was diluted to final dilutions of 1:10 and 1:100 in cell-free dilution plates by taking 30 μL of SNB-19 supernatant and diluting into 270 μL of complete DMEM (at a final concentration of 1:10), mixing, and taking 30 μL of the 1:10 mixture and diluting into another 270 μL of complete DMEM (at a final concentration of 1:100). Then, 100 μL from the cell-free dilution plates were added to the naïve Vero cell plate after removal of maintenance media, as seen in *Figure 1b*. This step allows an appropriate viral dilution range where the viral colonies can be counted, and can be adjusted as necessary, as it is important to note that neither manual nor automated colony counting can be accurately carried out if colony density is too high. After 2 h of incubation, the viral inoculum was removed, and 100 μL of methyl-cellulose overlay added to each well, and cells were incubated for 48 h at 37°C. The methyl-cellulose overlay was then removed by aspiration, wells were gently washed with phosphate buffered saline (PBS), and wells fixed with 100 μL 4% paraformaldehyde for 15 min, followed by three PBS washes. Cells were then blocked with 100 μL PBS with Triton X-100, normal goat serum, and bovine serum albumin (PBTG) (PBS containing 0.1% Triton X-100, 10% normal goat serum, and 1% bovine serum albumin) for 1 h at room temperature while rocking. Blocking solution was removed, and wells were incubated with 50 μL primary antibody solution (Clone 4G2, 1:500 in PBTG) at 4°C overnight while rocking. The next day, the cells were washed gently with 200 μL per well PBS three times, and then incubated with 50 μL secondary antibody solution (goat antimouse-IgG HRP, 1:500 in PBTG) for 1 h at room temperature. Cells were then washed with 200 μL per well PBS three times and incubated with 50 μL freshly prepared DAB solution per well for 10 min, before rinsing with deionized water (DAB prepared with nickel according to manufacturer's instructions).

Automated Image Acquisition

Clear bottom 96-well plates were imaged on an IN Cell 6000 automated high-content microscope (GE Health Care, Issaquah, WA). Whole-well images were captured using a 2×0.1 NA lens using brightfield (595 excitation and 706/72 emission) at 50 ms exposure and images were binned at 2×.

Table 1. Assay Protocol for Semiautomated ZIKV Titer Assay

Step	Parameter	Value	Description
(a) Compound treatment and ZIKV inoculation in SNB-19 cells			
1	Seed cells in plate	100 μL/well, 15,000 cells/well, RPMI-1640 media with 10% FBS and 1% antibiotics	In a sterile corning 96-well plate
2	Incubation	24 h	37°C, 5% CO_2
3	Compound dilution	0.9 μL of 10 mM compound stock in 300 μL/well (RPMI-1640% +10% FBS), 8 dilutions (including 0 μM) 3 × fold, 12 unique compounds per 96-well plate	In a sterile corning 96-well plate; 0–30 μM
4	Compound addition	Add 100 μL/well from step (3) to SNB-19 cells from step (1)	37°C, 5% CO_2 for 1 h
5	Virus addition	Inoculate SNB-19 cells from step (4) with virus at MOI = 0.5–1.	Use high-titer virus to avoid diluting drug concentration further
6	Incubation	24 h	37°C, 5% CO_2
7	Collection of viral supernatant from SNB-19 cells	100 μL/well	Freeze in sealed 96-well plates or use immediately for titration on Vero cells *(b)*.
(b) Titration in Vero cells			
1	Seed cells in plate	100 μL/well, 10,000 cells/well, DMEM with 10% FBS, 1% NEAA, 1% antibiotics	In a sterile corning 96-well plate; aim for confluent monolayer next day.
2	Incubation	24 h	37°C, 5% CO_2
3	Viral supernatant (SN) dilution	1:10 and 1:100 dilution of virus (optional: may include 1:1,000 if doing duplicates instead of triplicates)	In a sterile corning 96-well plate. 1:10—Add 33 μL of viral SN to 297 μL complete DMEM. Mix well, remove 30 μL, and add to 270 μL complete DMEM (1:100). Repeat once more for 1:1,000
4	First incubation	2 h	37°C, 5% CO_2
5	Methyl-cellulose overlay	100 μL/well	Equal parts 2X DMEM (2X DMEM +4% FBS) and 4% methyl-cellulose
6	Incubation	48 h	37°C, 5% CO_2
(c) Immunocytochemistry			
1	Fixation	100 μL/well 4% paraformaldehyde, 15 min at room temperature	Remove media, wash with PBS, and add 4% paraformaldehyde to fix
2	Wash	200 μL/well 1 × PBS	Wash 3 × with 1 × PBS
3	Block	50 μL/well PBTG for 1 h rocking at room temperature	PBTG: 1 × PBS
4	Primary antibody	50 μL/well antiflavivirus envelope D1-4G2-4-15 diluted in PBTG (1 mg/mL, diluted 1:500) for 1 h rocking at room temperature or 4°C overnight	ATCC: D1-4G2-4-15
5	Wash	200 μL/well 1 × PBS	Wash 3 × with 1 × PBS

(*continued*)

Table 1. *Continued*

Step	Parameter	Value	Description
6	Secondary antibody	50 μL/well goat antimouse HRP diluted in PBTG (1:500) for 1 h rocking at room temperature	Abcam: ab6789
7	Wash	200 μL/well 1 × PBS	Wash 3 × with 1 × PBS
8	DAB stain	50 μL/well, prepared per manufacturer's instructions, with nickel	10 min incubation followed by rinse with deionized water. Vector Labs: SK-4100
9	Image with IN Cell 2200 or IN Cell 6000		

ATCC, American Tissue Culture Collection; HRP, horse radish peroxidase; FBS, fetal bovine serum; MOI, multiplicity of infection; DMEM, Dulbecco's modified Eagle's medium; PBS, phosphate buffered saline; PBTG, phosphate buffered saline with Triton X-100, normal goat serum, and bovine serum albumin; DAB, diaminobenzidine.

Plate Blocker Usage for Clear Plates

A clear polystyrene plate lid was used to generate a plate blocker. The 96-well plate mask was drawn in Solid Works 3D software, saved as a .DWG file, imported to Corel then sent to the Fusion Epilog 50 watt laser, which was set up as a printer from the Corel software. The printer software allowed the vector cutting of a 6-mm diameter well pattern at 13% speed and 30% power. After cutting the lid, it was spray painted black.

Image Analysis and Optimization

Whole-well brightfield images were analyzed using IN Cell Developer 1.9.2 software (GE Health Care). Colonies were identified using intensity thresholding (typically 1,500–2,500 min and max intensity cutoffs) with three postprocessing steps (a sieve to retain objects >300 μm, a three-kernel dilation step to join objects, and a border removal screen to remove edge-of-well signal from the clear wells). Intensity thresholding was performed manually per run-based positive and negative control wells with typical minimum and maximum values at ~1,500–2,500 gray levels, respectively. Analysis was conducted on a 24 core HP Z840 workstation with 32 GB of RAM running Windows 7.

IC_{50} Calculation and Plotting

All data points were input into Graph Pad Prism (version 7) for dose–response curve fitting and determination of IC_{50}. The 0 μM was graphed as 0.01 μM for dose–response curve for each compound. IC_{50} values were generated using nonlinear regression and the "log(inhibitor) versus response—Variable slope (four parameters)" function. All IC_{50} values were further validated by subsequent eye analysis of dose–response curves.

RESULTS

We established a standard protocol consisting of two parts: compound titration/viral focus formation and automated imaging/data analysis. We first chose 139 unique compounds that showed antiviral activity in a high-throughput, anti-ZIKV replication-based compound screen, which utilized a Zika NS1-FRET-based assay (data unpublished). Using these compounds, we then treated a physiologically relevant cell line, the human glioblastoma cell line SNB-19 in individual experiments with each compound, up to 12 compounds per plate, each with a titration range of 0–30 μM (for a total of eight concentrations for each compound), before Zika virus infection (schematic shown in *Fig. 1A*). After infecting the drug-treated Vero cells with ZIKV, infectious virion production was then measured by a focus-forming unit assay on naïve Vero cells (schematic shown in *Fig. 1B, C*), which are highly susceptible to a broad range of viral infections.[8] Traditionally, the resulting foci would be manually counted either by naked eye or under microscope. However, to analyze a large number of compounds and resulting titer plates, we developed a rapid automated imaging and analysis workflow. We chose nine of these previously unpublished compounds from the ZIKV-NS1 FRET-based assay, plus the previously published niclosamide,[9] for side-by-side comparison of automated versus manual colony counting for developing and validating our rapid automated imaging analysis protocol, to demonstrate that our protocol is capable of producing reliable colony counts comparable with traditional manual counts (*Fig. 1D, E*) (R^2 values >0.95).

Viral Titration Assay

The first step of the modified viral titer assay is compound titration and viral infection. Twelve compounds were serially

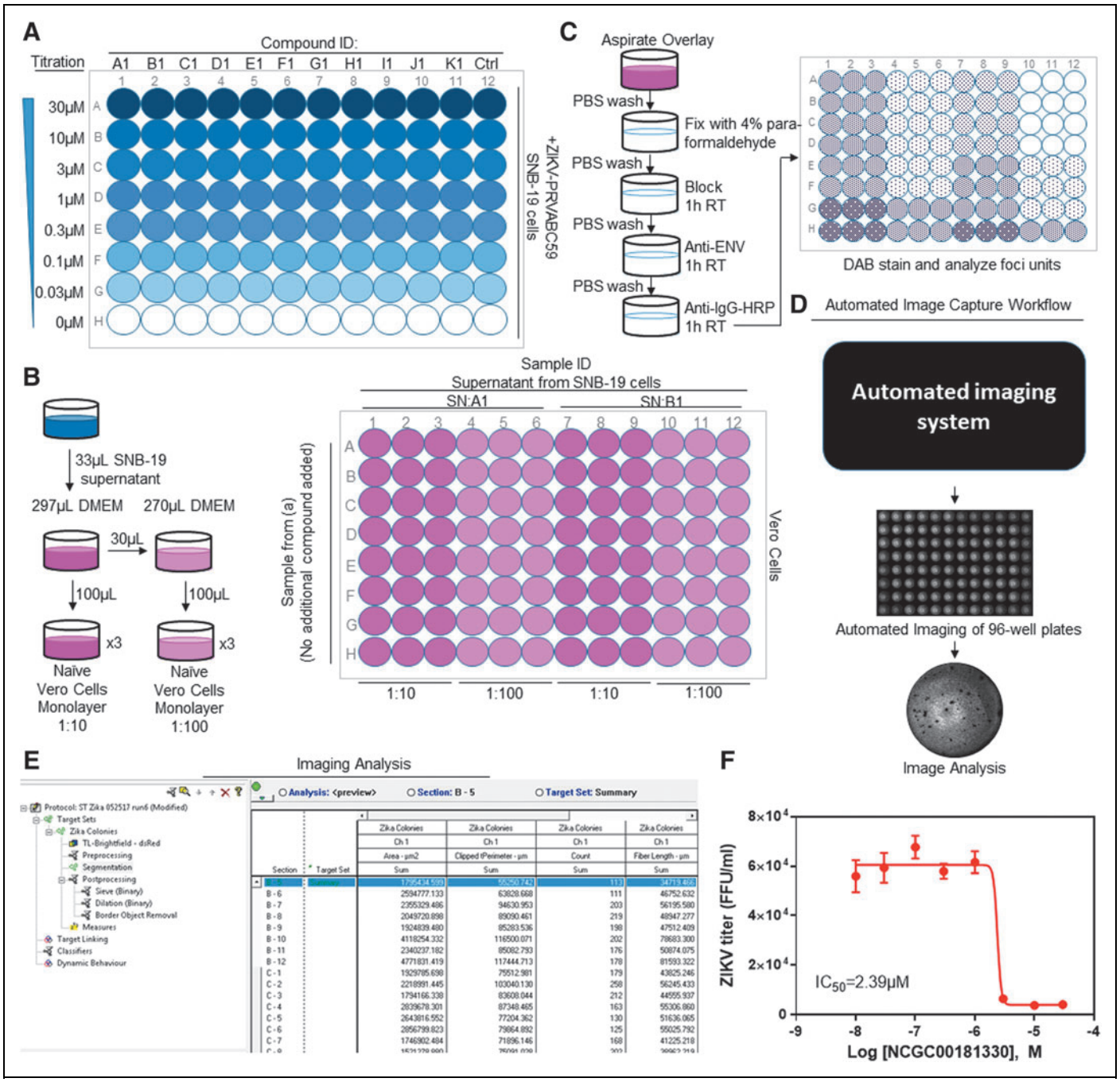

Fig. 1. Experimental flow chart of ZIKV titer assay. **(A)** Compound dilution in SNB-19 cells followed by ZIKV infection for 24 h. **(B)** Infection of Vero cells for ZIKV titer assay. ZIKV-infected SNB-19 cell supernatant from **(A)** was diluted and incubated with naïve Vero cells. **(C)** Cell fixation, staining for Zika viral antigen, and focus-forming unit detection using DAB substrate. **(D)** Automated imaging acquisition. **(E)** Protocol in the IN Cell Developer software (GE Health Care). **(F)** Concentration–response curve fitting for IC_{50} calculation. DAB, diaminobenzidine.

diluted per 96-well plate, with eight, threefold dilutions per unique compound (from 30 to 0 μM), and then added to SNB-19 cells for a 1 h preincubation (*Fig. 1A*), followed by inoculation with the clinical isolate PRVABC59-ZIKV at MOI of 0.5. After a 24 h incubation, supernatants in the assay plates were immediately diluted and used to inoculate naïve Vero cells cultured in a 96-well plate for the focus-forming unit assay. Alternatively, the viral-infected SNB-19 supernatants could be transferred into a new 96-well plate, sealed, and frozen at –80°C for later use. The second step is the focus-forming

unit assay. Vero cells were inoculated with the viral-infected SNB-19 cell supernatant in triplicates at a minimum of two dilutions (1:10 or 1:100) to ensure a suitable countability range (defined by maximum achievable number of well-defined and distinct colonies) of focus-forming units (*Fig. 1B*). After 2 h, cell supernatants were removed, and cells were covered with a methyl-cellulose overlay to prevent newly secreted viruses from diffusing through cell-culture media, thus minimizing secondary rounds of cell-free infection. After 48 h, the Vero cells were fixed, stained for ZIKV antigen, and visualized using DAB (+nickel) substrate (*Fig. 1C*). All dilutions and transfers were carried out with electronic multichannel pipettes to increase the speed of the titration process, as described in the Methods section. These steps can be fully automated with a robotic system.

Automated Imaging

The third step is the imaging and quantification of infection foci. Traditionally, the resulting focus-forming units are quantified manually, either by naked eye if the foci are large enough or under a microscope. To improve upon this workflow, we employed an automated imaging system to capture whole-well images in the 96-well assay plate (*Fig. 1D*). Using the IN Cell 6000 automated high-content microscope, we captured

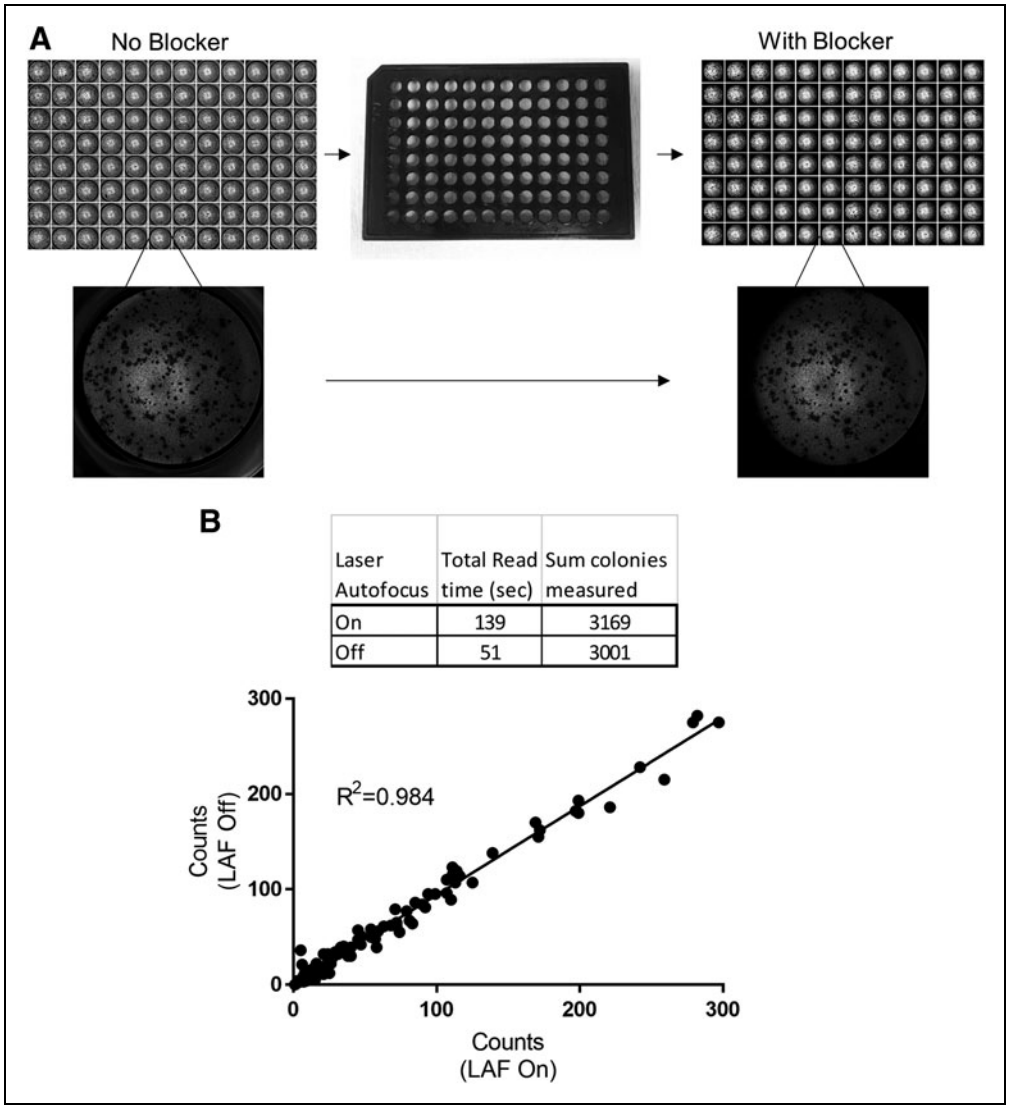

Fig. 2. Use of 96-well plate blocker to remove out of well transmitted light scatter from wells. **(A)** *Top left* and *right*: Montage images of a 96-well plate before and after plate blocker usage. *Center*: image of plate blocker used. *Bottom left* and *right*: images of wells captured before and after blocker. **(B)** Comparison of automated image acquisition modalities from a 96-well plate; effects of laser autofocus on acquisition speed and colony count.

whole-well images by applying a 2×0.1 NA lens using brightfield (595 excitation and 706/72 emission) at 50 ms exposure.

The 96-well plates used for screening were completely transparent, and therefore exhibited edge-well and out-of-well signal when captured using a whole-well imaging and brightfield excitation.

To remove this background noise and optimize automated colony counting, we imaged plates using a customized plate blocker (*Fig. 2A*). To optimize acquisition speed, we imaged plates with and without laser autofocus (LAF). When imaging without LAF, the focal plane was set at 2,990 µm. When using LAF, the optimal focus offset from plate bottom was 129 µm, and the average bottom height was found at 2861.9 µm with a standard deviation of 46.5 µm. Total plate read time with LAF turned on was 139 s, and that with LAF turned off was 51 s. Total colonies measured in the plate were 6,353 and 6,013 with LAF on and off, respectively. By turning off LAF during acquisition, we improved read times by 63% with a correlation of colony count identification 98.4% between LAF on and off (*Fig. 2B*). The overall workflow is outlined in *Figure 1 and Table 1*.

Automated Analysis

The images of individual wells captured by the IN Cell 6000 automated high-content microscope were at significantly higher resolution compared with those observed in the manual experiment with a standard Canon EOS camera. Images taken by the standard Canon EOS were taken only for initial comparison purposes to represent the traditional manual counting process (*Fig. 3A, B*). Once images were captured, individual colony counts were quantitated by automated analysis using the IN Cell Developer image analysis software (*Fig. 3D*). To compare the results from automated counting with those from manual counting, we selected the wells with well-separated colonies for analysis (*Fig. 3C*). We examined multiple image

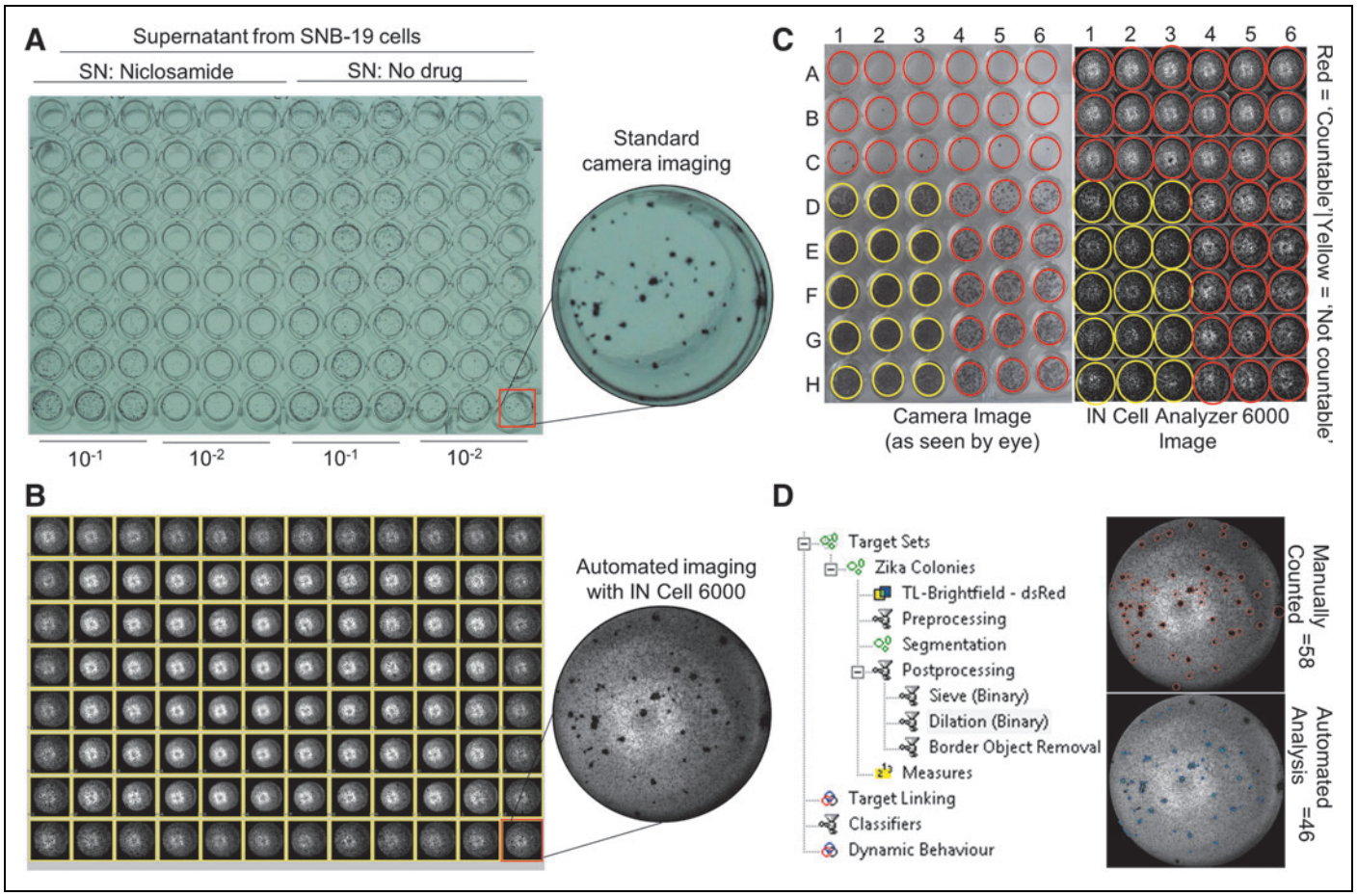

Fig. 3. Images of 96-well plates and colonies in the ZIKV titer assay. **(A)** Image taken manually using a handheld Canon EOS Rebel T6 digital camera. **(B)** Image taken using automated imaging acquisition with the IN Cell Analyzer 6000. **(C)** "Countable" versus "not-countable" wells. **(D)** Automated colony analysis using the HP z840 24 core machine for quantification of ZIKV titer in 96-well plates.

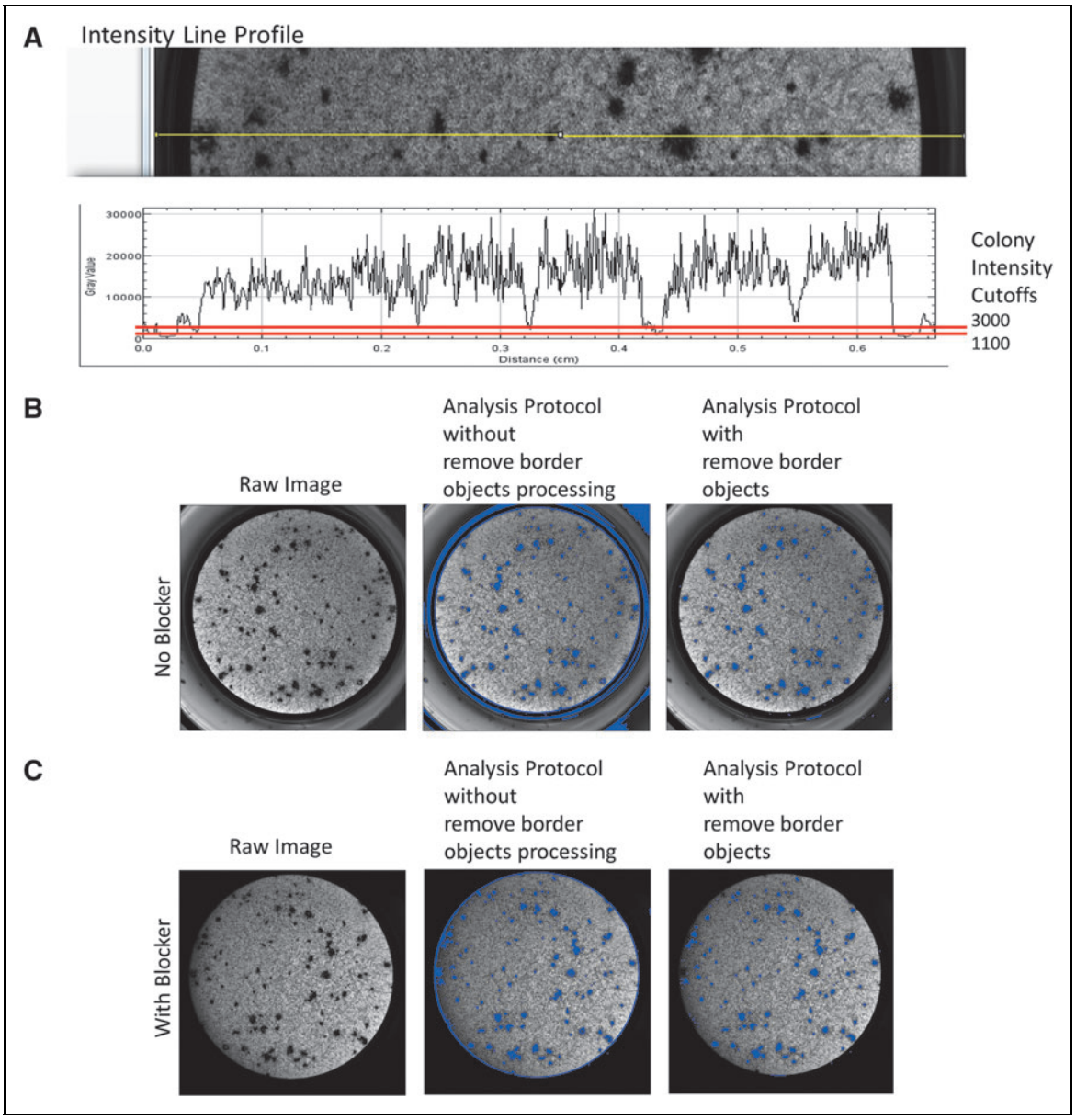

Fig. 4. Artifact removal. **(A)** Intensity line profile plot of image acquired without blocker. *Yellow line* indicates position of profile line used in plot. *Red lines* indicate intensity cutoff criteria used to identify and segment colonies. **(B, C)** Ninety-six-well plate image without and with (respectively) plate blocker and resulting image analysis.

analysis algorithms and compared the results with those determined by the traditional manual colony counts. Standard "canned" algorithms in the GE software package are designed to analyze fluorescence signals (i.e., gain of signal over a lower background). The brightfield images acquired have a range of signals with background on either side of the intensity scale. We found that the canned algorithms did not adequately identify DAB-stained colonies imaged with brightfield, and therefore generated a custom analysis protocol using signal intensity criteria described below.

When brightfield imaging was used to capture whole-well images, the typical intensity values of DAB-stained colonies were on the order of ~1,500–2,500 grayscale values (on a range of 65,536 from the 16-bit camera sensor). The analysis protocol used 1,100 to 3,000 gray levels as intensity cutoffs with three postprocessing steps (*Figs. 1E and 4A*). To alleviate artifacts (such as debris and edge-of-well false signals), several postprocessing steps were employed: a sieve to remove small debris and retain objects >1,000 μm, a dilation step of three kernels to join objects within colonies, and a border objects removal step to eliminate

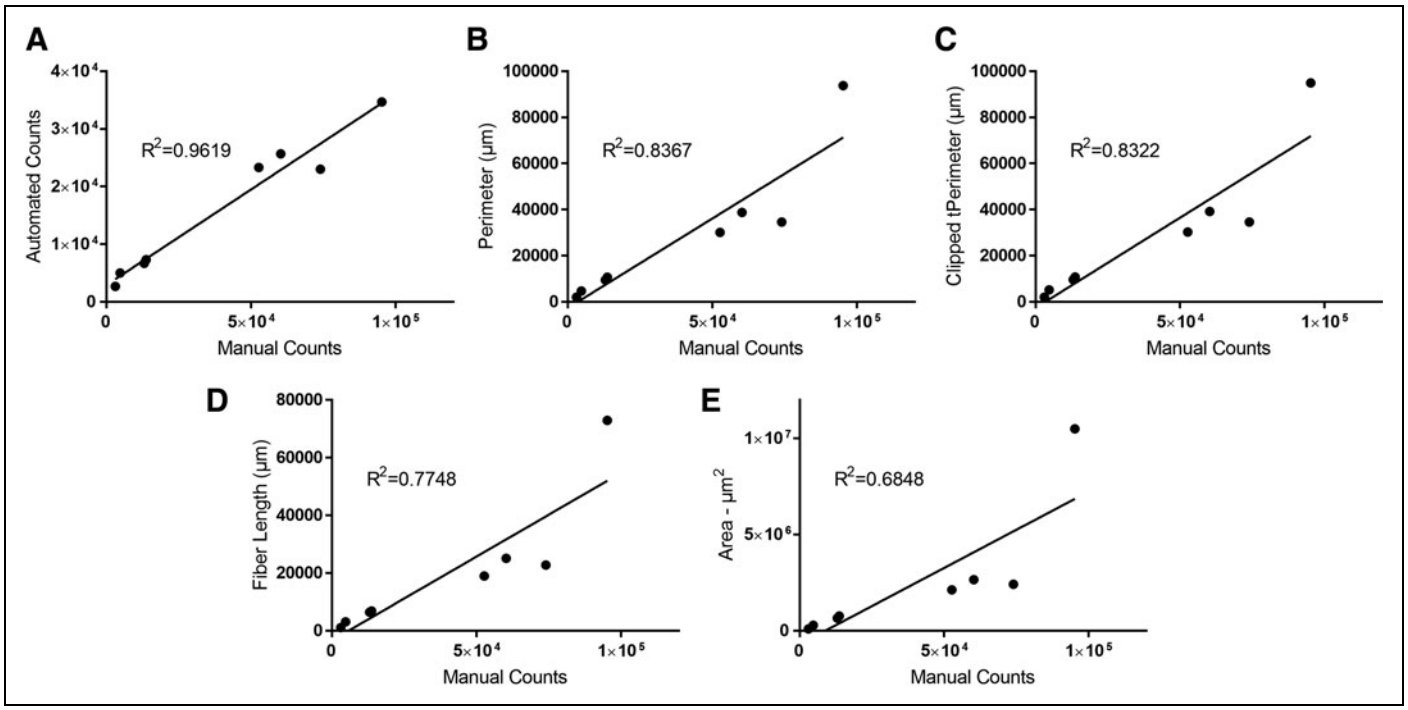

Fig. 5. Comparison plots of manual colony counts to automated image analysis parameters. A 96-well plate treated with two unique compounds at eight drug doses (including o µM) and two viral dilutions was imaged and analyzed using manual or automated imaging. The X-axis represents manual colony counts; each point represents the average number of colonies per well ($n = 3$). Automated parameters on the Y-axis measures included **(A)** colony counts, **(B)** total colony perimeter per well, **(C)** total clipped perimeter, **(D)** total fiber length (processes extending from colony bodies), and **(E)** total colony area.

edge-of-well artifacts. After utilizing these processes and the use of a plate blocker to minimize edge-well artifacts (*Figs. 2A, 4B, C*), correlation between manual and automated colony counts was ~90%. In addition, we tested several parameters to compare IC_{50} values of standard compounds with their counterpart IC_{50} values determined by the manual counting method. These parameters include automated colony counts, total colony perimeter, total colony area, total fiber length, plate cover type, and clipped total perimeter (*Fig. 5*). Of these, the IC_{50} values generated from automated colony quantification, total colony counts, and total colony area had the strongest correlation to those determined by the traditional manual counting. The optimized analysis protocol had R^2 values >0.95 over 12 plates as compared with the traditional manual colony-counting method (*Fig. 5A*).

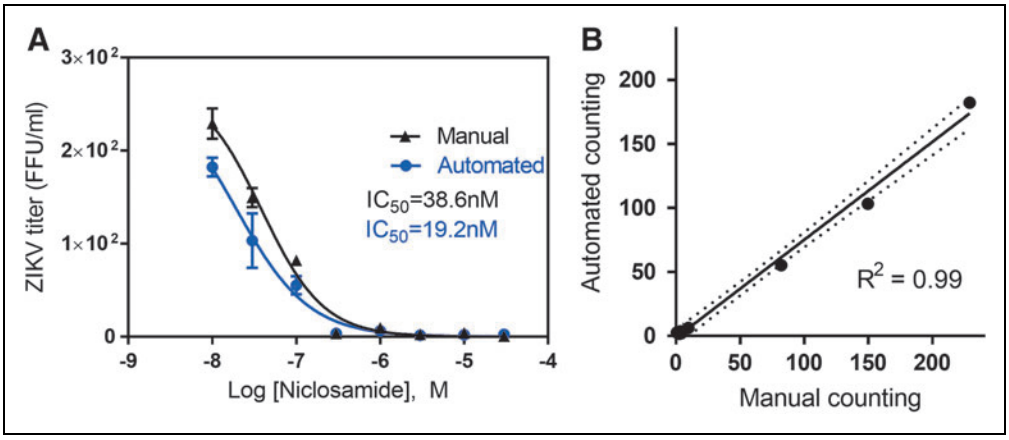

Fig. 6. Correlation of IC_{50} values of anti-ZIKV compounds between the high-throughput ZIKV titer assay and the ZIKV automated assay. **(A)** Concentration–response curves and IC_{50} values of niclosamide determined in the manual versus automated ZIKV titer assay. **(B)** Correlation of manual versus automated colony counting from niclosamide data seen in **(A)**.

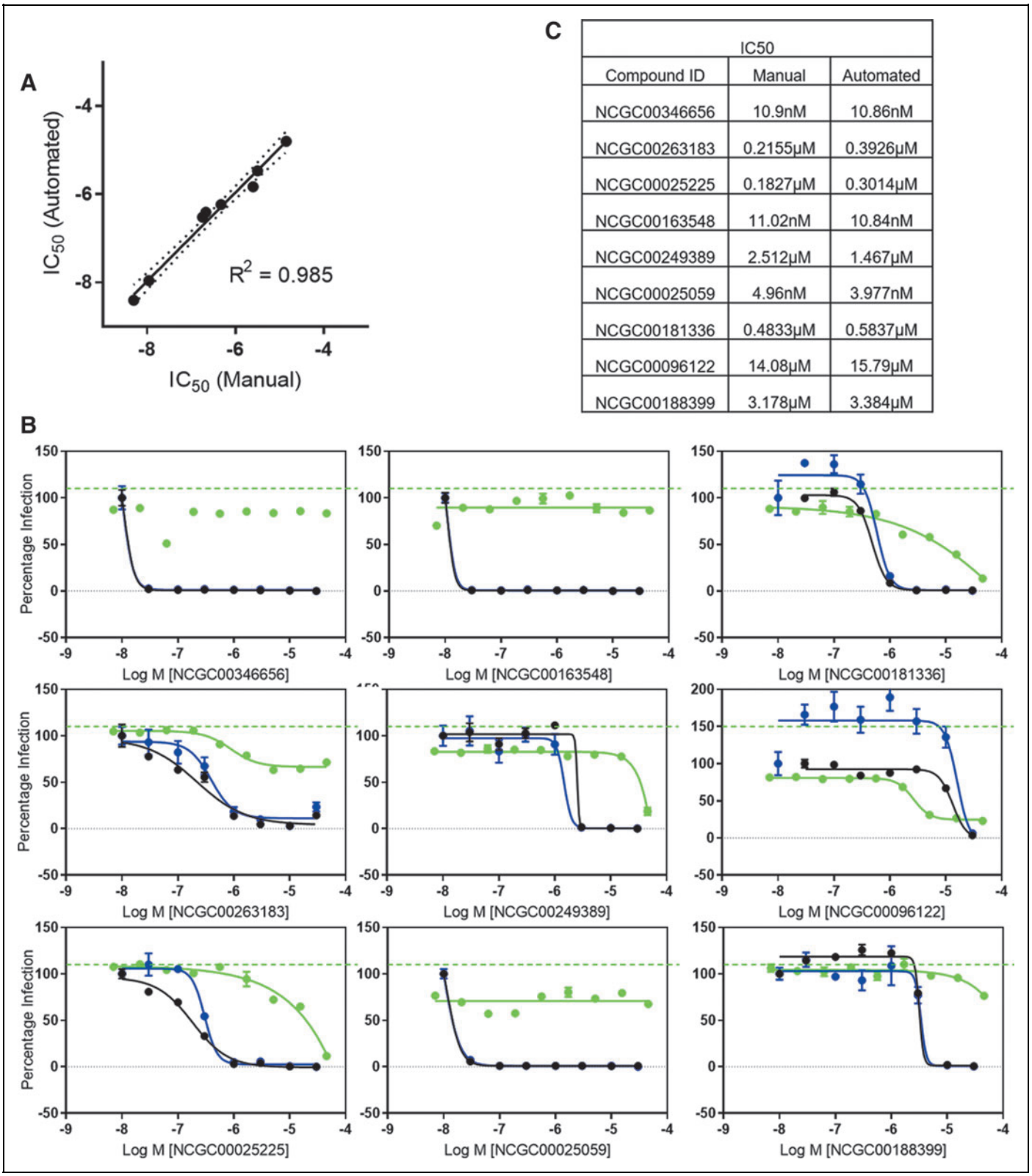

C

IC50		
Compound ID	Manual	Automated
NCGC00346656	10.9nM	10.86nM
NCGC00263183	0.2155μM	0.3926μM
NCGC00025225	0.1827μM	0.3014μM
NCGC00163548	11.02nM	10.84nM
NCGC00249389	2.512μM	1.467μM
NCGC00025059	4.96nM	3.977nM
NCGC00181336	0.4833μM	0.5837μM
NCGC00096122	14.08μM	15.79μM
NCGC00188399	3.178μM	3.384μM

Fig. 7. Comparison of IC_{50} values across nine active compounds from manual and automated colony-counting methods. **(A)** Correlation of IC_{50} measurements generated from manual versus automated colony counting for nine unique compounds. **(B)** IC_{50} graphs generated for nine active compounds by manual and automated colony-counting methods. **(C)** Table of IC_{50}'s from nine active compounds in **(B)**. *Black lines* represent manual counts. *Blue lines* represent automated counts. Compound toxicity (without viral infection) is represented by the *green solid line*.

We further validated our automated ZIKV titer counts by comparing both the raw counts and the calculated IC_{50} values generated from two sets of experiments. First, we tested the calculated IC_{50} value of a previously reported anti-ZIKV compound, niclosamide.[9] Manual analysis yielded an IC_{50} of 38.6 nM, whereas automated analysis produced an IC_{50} of 19.2 nM (*Fig. 6A*). Regression analysis of automated colony count versus manual colony count yielded a R^2 value of 0.99 (*Fig. 6B*). Second, we tested nine previously unpublished compounds for anti-ZIKV activity by focus-forming unit assay, and compared results from the two methods regarding viral titers and IC_{50} values (*Fig. 7A–C*). A correlation analysis of the IC_{50} values determined by automated colony counting compared with these by manual colony counting yielded a R^2 value of 0.985 in the regression line (*Fig. 7A*). Collectively, the data indicate that this automated colony-counting method is a valid replacement to the manual counting assay.

DISCUSSION

We have described an improved, more efficient method for the traditional viral titer assay in a semiautomated, higher throughput setting. It overcomes the shortcomings of labor intensiveness and human bias in the traditional viral titer assay.[7] With automated image capture and analysis, the throughput of this screen is greatly increased. Typically, it takes 50 s for the automated image acquisition and 1 min for the automated colony analysis for a 96-well plate, resulting in a throughput of 30–40 plates per hour for the imaging acquisition and colony counting. The rate-limiting steps in this method are the cell plating, compound dilution, addition to supernatant cell plate, and viral inoculation, and titration. However, these rate-limiting steps can be easily improved using a fully automated robot with automated liquid dispensers and an automated plate washer.

There are several reported high-throughput assays and reporter viruses for anti-ZIKV compound discovery.[9–14] While these assays are critical in their ability to screen in high throughput for drugs that block ZIKV infection, these assays are based on viral replication, single-round culture infection, or ZIKV-induced cell cytotoxicity. None currently utilize an infectious virion production-based assay such as the focus-forming unit assay, which is a viral assay that encompasses the full viral life cycle. One potential shortcoming of a solo infectious virion production-based assay is that it lacks an internal control for compound cytotoxicity. However, this can easily be addressed by including a parallel screen for compound toxicity using established toxicity assays such as ATP-content assay,[15] as shown in *Figure 7C*. Whereas we do not see input viral inoculum carryover in the titer assay, most likely as a result of the relatively short half-life of infectious ZIKV particles in cell culture at 37°C, it is possible that there may be input drug carryover in the assay.[16] While we have not observed significant effect of compound carryover in our compound study, expanding the infectious virion dilution range in combination with using a higher initial MOI during the initial drug screening may help reduce potential drug carryover.

Because we use automated imaging and analysis based on immunolabeled viral foci, the modified viral titer assay workflow we describe here can easily be adapted to other viruses for which there are established focus-forming unit assays. Importantly, the time points chosen for assessing viral titer can be adjusted per virus. For ZIKV, we chose to assay viral production at 24 h postinfection, as we routinely observed robust viral production at this time point. However, this time point can be optimized depending on the life cycle kinetics of the virus being tested.

In the ZIKV titer assay described, we were able to develop a streamlined workflow, including automated whole-well image capture and an image-based algorithm, to accurately generate automated colony counts with a R^2 value of 0.99 when compared with traditional manual counts. In addition, our automated colony counts robustly generated IC_{50} values for nine individually tested compounds, yielding a R^2 value of 0.985 in the regression line when compared with those generated by manual counts. In addition to the increased throughput of our modified ZIKV titer assay, another distinct advantage of an automated high-throughput viral titer assay is that it is image based rather than signal based, removing compound interference and assay artifacts such as compound autofluorescence or quenching.[17] In addition, each identified viral focus can be characterized based on a set of parameters that are adjustable according to desired viral foci characteristics. Thus, this assay is well suited for use as an orthogonal assay for confirming antiviral hits generated from high-throughput screens utilizing fluorescence or luciferase as a readout.

Overall, our modified, high-throughput designed infectious virion production and automated imaging workflow is a useful tool for validating hits from these initial high-throughput antiviral screens. In our ZIKV NS1-FRET-based assay, we validated 78 of 256 initial hits as positive for anti-ZIKV activity <1 μM concentration. The automation of the classical viral titration assay will greatly assist in discovery and development of potential anti-ZIKV compounds.

ACKNOWLEDGMENTS

This work was supported by the Intramural Research Program of the National Center for Advancing Translational Sciences, National Institutes of Health (W.Z.) and by Public Health Service Grants U19 AI131130 and R21 AI119530 (H.T.).

AUTHORS' CONTRIBUTIONS

W.Z. and H.T. conceived the project. E.L. optimized and carried out virus titration assays and analysis of counts. S.T. designed and optimized imaging conditions and software analysis. M.X. screened and identified potential anti-ZIKV drugs from a high-throughput screen for use in the viral titration assay. E.L., S.T., and W.Z. prepared figures and wrote the article. E.L. and S.T. contributed equally to this work.

DISCLOSURE STATEMENT

No competing financial interests exist.

REFERENCES

1. World Health Organization: Zika situation report. March 10, 2017. Available at: https://www.who.int/emergencies/zika-virus/situation-report/10-march-2017/en/ (Last accessed on February 28, 2019).
2. Mlakar J, Korva M, Tul, N, *et al.:* Zika virus associated with microcephaly. *N Engl J Med* 2016;374:951–958.
3. Rasmussen SA, Jamieson DJ, Honein MA, Petersen LR: Zika virus and birth defects—reviewing the evidence for causality. *N Engl J Med* 2016;374:1981–1987.
4. Cao-Lormeau VM, Blake A, Mons S, *et al.:* Guillain–Barré syndrome outbreak associated with Zika virus infection in French Polynesia: a case–control study. *Lancet* 2016;387:1531–1539.
5. Araujo LM, Ferreira ML, Nascimento OJ: Guillain–Barré syndrome associated with the Zika virus outbreak in Brazil. *Arq Neuropsiquiatr* 2016;74:253–255.
6. Fontes CA, Dos Santos AA, Marchiori E: Magnetic resonance imaging findings in Guillain–Barré syndrome caused by Zika virus infection. Neuroradiology 2016; 58:837–838.
7. Fields BN, Knipe DM, Howley PM: *Fields virology*. Philadelphia, PA, Wolters Kluwer Health/Lippincott Williams & Wilkins, 2013.
8. Rhim JS, Schell K, Creasy B, Case W: Biological characteristics and viral susceptibility of an African Green Monkey Kidney Cell Line (Vero). *Exp Biol Med* 1969;132:670–678.
9. Xu M, Lee EM, Wen Z, *et al.*: "Identification of small-molecule inhibitors of Zika virus infection and induced neural cell death via a drug repurposing screen." *Nat Med* 2016;22:1101–1107.
10. Barrows NJ, Campos RK, Powell ST, *et al.*: "A screen of FDA-approved drugs for inhibitors of Zika virus infection." *Cell Host Microbe* 2016;20:259–270.
11. Müller JA, Harms M, Schubert A, *et al.*: "Development of a high-throughput colorimetric Zika virus infection assay." *Med Microbiol Immunol* 2017;206: 175–185.
12. Adcock RS, Chu Y, Golden JE, Chung D. "Evaluation of Anti-Zika virus activities of broad-spectrum antivirals and NIH clinical collection compounds using a cell-based, high-throughput screen assay." *Antiviral Res* 2017;138:47–56.
13. Xie X, Zou J, Shan C, *et al.*: "Zika virus replicons for drug discovery." *EBioMedicine* 2016;12:156–160.
14. Zhou T, Tan, Cederquist GY, *et al.*: "High-content screening in HPSC-neural progenitors identifies drug candidates that inhibit Zika virus infection in fetal-like organoids and adult brain." *Cell Stem Cell* 2017;21:274–283.e5.
15. Kouznetsova J, Sun W, Martinez-Romero C, *et al.*: "Identification of 53 compounds that block Ebola virus-like particle entry via a repurposing screen of approved drugs." *Emerg Microbes Infect* 2014;3:e84.
16. Goo L, Dowd KA, Smith AR, *et al.*: "Zika virus is not uniquely stable at physiological temperatures compared to other flaviviruses." *MBio* 2016;7:5.
17. Simeonov A, Davis MI: "Interference with fluorescence and absorbance." In: *Assay Guidance Manual*. Sittampalam GS, Coussens NP, Nelson H, *et al.* (eds.). Bethesda, MD, Eli Lilly & Company and the National Center for Advancing Translational Sciences, 2015: Available at: www.ncbi.nlm.nih.gov/books/NBK343429.

Address correspondence to:
Hengli Tang, PhD
Department of Biological Science
Florida State University
319 Stadium Drive
Tallahassee, FL 32306

E-mail: tang@bio.fsu.edu

Wei Zheng, PhD
National Center for Advancing Translational Sciences
National Institutes of Health
9800 Medical Center Drive
Rockville, MD 20850

E-mail: wzheng@mail.nih.gov

Abbreviations Used

ATCC = American Tissue Culture Collection
DAB = diaminobenzidine
DMEM = Dulbecco's modified Eagle's medium
FBS = fetal bovine serum
FFA = focus-forming assay
HRP = horse radish peroxidase
IgG = immunoglobulin G
LAF = laser autofocus
MOI = multiplicity of infection
PBS = phosphate buffered saline
PBTG = phosphate buffered saline with Triton X-100, normal goat serum, and bovine serum albumin
PSA = penicillin–streptomycin-amphotericin B
ZIKV = Zika virus